Evaluation of the forward Compton scattering off protons: II. Spin-dependent amplitude and observables

Oleksii Gryniuk, Franziska Hagelstein, and Vladimir Pascalutsa

Institut für Kernphysik and PRISMA Cluster of Excellence,
Johannes Gutenberg-Universität Mainz, D-55128 Mainz, Germany

(Dated: September 7, 2016)

The forward Compton scattering off the proton is determined by substituting the empirical total photoabsorption cross sections into dispersive sum rules. In addition to the spin-independent amplitude evaluated previously [Phys. Rev. D **92**, 074031 (2015)], we obtain the spin-dependent amplitude over a broad energy range. The two amplitudes contain all the information about this process, and we, hence, can reconstruct the nonvanishing observables of the proton Compton scattering in the forward kinematics. The results are compared with predictions of chiral perturbation theory where available. The low-energy expansion of the spin-dependent Compton scattering amplitude yields the Gerasimov-Drell-Hearn (GDH) sum rule and relations for the forward spin polarizabilities (FSPs) of the proton. Our evaluation provides an empirical verification of the GDH sum rule for the proton, and yields empirical values of the proton FSPs. For the GDH integral, we obtain $204.5(21.4)$ μb, in agreement with the sum rule prediction: $204.784481(4)$ μb. For the FSPs, we obtain: $\gamma_0 = -92.9(10.5)\times10^{-6}$ fm^4, and $\bar\gamma_0 = 48.4(8.2)\times10^{-6}$ fm^6, improving on the accuracy of previous evaluations.

PACS numbers: 13.60.Fz - Elastic and Compton scattering, 14.20.Dh - Protons and neutrons, 25.20.Dc - Photon absorption and scattering, 11.55.Hx Sum rules.

arXiv:1604.00789v2 [nucl-th] 6 Sep 2016

I. INTRODUCTION

The forward Compton scattering (CS) off a spin-1/2 target, such as the nucleon, is described by two complex functions of the photon energy ν: the spin-independent amplitude, $f(\nu)$, and the spin-dependent amplitude, $g(\nu)$. The general requirements of unitarity and causality allow one to express these amplitudes in terms of integrals of total photoabsorption cross sections [1] (see Refs. [2, 3] for reviews). At least for the proton, these cross sections are fairly well known by now, and, whereas in the previous paper [4] we obtained the *spin-independent* amplitude, here we evaluate the *spin-dependent* one. Having both of them, we can reconstruct all observables of the forward CS off the proton.

This is essentially the only way to access the forward CS observables empirically — a direct observation of strictly forward CS is not possible in practice. Indirectly, the forward CS can be measured through dilepton photoproduction, where the timelike CS enters prominently in certain kinematics, while the photon virtuality is small (quasireal CS). However, the only experiment of this kind was done at DESY in 1973 [5], measuring the spin-independent amplitude f at 2.2 GeV.

The spin-dependent amplitude $g(\nu)$ has not yet been measured through the dilepton photoproduction and not much is known about it empirically. Until now, only its low-energy expansion has been studied. The leading-order term yields the Gerasimov–Drell–Hearn (GDH) sum rule [6, 7], which has recently been verified for the proton by the GDH Collaboration [8–11]. The forward spin polarizability (FSP) sum rules, arising at the next two orders, have been evaluated by Pasquini *et al.* [12]. In this work, having evaluated $g(\nu)$ over a broad energy range, we, too, consider its low-energy expansion and hence reevaluate the sum rules. The results are compared with the previous evaluations in Table II.

The results for the energy dependence of the amplitude $g(\nu)$ and the observables can be compared with theoretical calculations. At low the energies we shall compare to the calculations based on chiral perturbation theory (χPT). More specifically, in the lower panels of Figs. 3, 4, and 5, our results are compared to the calculations of Lensky *et al.* [13–15] done in the manifestly covariant baryon χPT (BχPT). Other state-of-art χPT calculations of proton CS, based on the heavy-baryon expansion (HBχPT) [16, 17], were shown [18] to be in agreement with the aforementioned BχPT calculation, within the estimated theoretical uncertainties. Therefore, in the figure, we only plot one of the two, whereas the forward spin polarizabilities can be compared to either of them in Table II.

An interesting issue arises when studying the elastic contribution to the sum rules in perturbative QED: the low-energy expansion, which goes into the sum rule derivation, is inapplicable. It is nonetheless possible to write down the elastic sum rules for both the spin-independent [4] and the spin-dependent cases as covered in the Appendix.

This paper is organized as follows. In Sec. II we give a brief overview of the Kramers-Kronig relations for the forward CS amplitudes and the sum rules involving the spin-dependent amplitude g. In Sec. III we describe the fitting procedure for the helicity-difference photoabsorption cross section. We then evaluate the sum rule integrals and the energy dependence of the spin-dependent amplitudes in Sec. IV, and present results for the forward CS observables in Sec. V. Conclusions are given in Sec. VI. In the Appendix we discuss the elastic contribution to the sum rules in spinor QED at one-loop level.

II. FORWARD COMPTON AMPLITUDE AND SUM RULES

The Lorentz structure of the *forward* CS amplitude for a spin-1/2 target, such as the nucleon, can be decomposed into two terms,[1]

$$T^{\mu\nu}(p,q) = -\left[\mathrm{g}^{\mu\nu} f(\nu) + \gamma^{\mu\nu} g(\nu)\right], \qquad (1)$$

[1] The tensors can in principle be written in an explicitly current-conserving form (i.e., such that $q_\mu T^{\mu\nu} = 0$); however, additional terms vanish when contracted with the photon polarization vector ε^μ, because of $q\cdot\varepsilon = 0$.

where $g^{\mu\nu} = \mathrm{diag}(1,-1,-1,-1)$ is the metric tensor and $\gamma^{\mu\nu} = \frac{1}{2}[\gamma^\mu, \gamma^\nu]$ is the antisymmetrized product of Dirac matrices. The amplitudes f and g are complex functions of the variable $\nu = p\cdot q/M$, with p and q being the target and photon 4-momentum; $p^2 = M^2$, $q^2 = 0$. The corresponding helicity amplitudes are found as

$$T_{\lambda'_\gamma \lambda'_N \lambda_\gamma \lambda_N} = \chi^\dagger_{\lambda'_N} \Big\{ f(\nu)\, \boldsymbol{\varepsilon}^*_{\lambda'_\gamma} \cdot \boldsymbol{\varepsilon}_{\lambda_\gamma} + g(\nu)\, i\, (\boldsymbol{\varepsilon}^*_{\lambda'_\gamma} \times \boldsymbol{\varepsilon}_{\lambda_\gamma}) \cdot \boldsymbol{\sigma} \Big\} \chi_{\lambda_N}, \tag{2}$$

where $\lambda_\gamma(\lambda'_\gamma)$ is the incoming (outgoing) photon helicity, $\lambda_N(\lambda'_N)$ is the incoming (outgoing) nucleon helicity, $\boldsymbol{\varepsilon}$ are the photon polarization vectors, and the Pauli spinors χ denote the target polarization. In terms of the total helicity $\Lambda = \lambda_\gamma - \lambda_N$, the amplitude is diagonal: $T_{\Lambda'\Lambda} = \delta_{\Lambda'\Lambda}\, \mathcal{T}_\Lambda$. Hence, there are only two independent helicity amplitudes: $\mathcal{T}_{\pm 3/2} = (f - g)$ and $\mathcal{T}_{\pm 1/2} = (f + g)$. The optical theorem (unitarity) relates the imaginary part of these amplitudes to the corresponding photoabsorption cross sections,

$$\mathrm{Im}\, \mathcal{T}_\Lambda(\nu) = \frac{\nu}{4\pi}\, \sigma_\Lambda(\nu), \tag{3}$$

with $\Lambda = 1/2, 3/2$. Rewriting these relations for f and g, one obtains the usual,

$$\mathrm{Im}\, f(\nu) = \frac{\nu}{8\pi} \left[\sigma_{1/2}(\nu) + \sigma_{3/2}(\nu)\right] \equiv \frac{\nu}{4\pi}\, \sigma(\nu), \tag{4a}$$

$$\mathrm{Im}\, g(\nu) = \frac{\nu}{8\pi} \left[\sigma_{1/2}(\nu) - \sigma_{3/2}(\nu)\right] \equiv -\frac{\nu}{8\pi}\, \Delta\sigma(\nu), \tag{4b}$$

where by σ and $\Delta\sigma$ we denote, respectively, the unpolarized and the helicity-difference cross sections of total photoabsorption.

Furthermore, the analytic and crossing properties of the amplitudes f and g, in conjunction with Eq. (4), allow one to write the following dispersion relations,

$$\mathrm{Re}\, f(\nu) = -\frac{Z^2\alpha}{M} + \frac{\nu^2}{2\pi^2} \fint_0^\infty \mathrm{d}\nu' \frac{\sigma(\nu')}{\nu'^2 - \nu^2}, \tag{5a}$$

$$\mathrm{Re}\, g(\nu) = -\frac{\nu}{4\pi^2} \fint_0^\infty \mathrm{d}\nu' \frac{\nu' \Delta\sigma(\nu')}{\nu'^2 - \nu^2}, \tag{5b}$$

where M is the nucleon mass and $Z = 1$ or 0 for the proton or neutron, respectively; the slashed integral denotes the principal-value integration. The dispersion relation for the spin-independent amplitude, f, was discussed in the previous paper [4]. Here, we focus on the spin-dependent amplitude, g, and the helicity-difference cross section, $\Delta\sigma$, for the proton.

We note that the cross sections include the CS process itself, as well as multiphoton production. We neglect those processes since they are of course suppressed by at least one order of α with respect to hadron-production processes, such as the pion photoproduction (more details on leading radiative corrections can be found in the Appendix). The cross sections which exclude electromagnetic radiation will be denoted by $\sigma_{\rm abs}$ and are assumed to begin with the lowest hadron-production threshold. We thus deal with the following relation for the spin-dependent forward CS amplitude,

$$\mathrm{Re}\, g(\nu) = -\frac{\nu}{4\pi^2} \fint_{\nu_0}^\infty \mathrm{d}\nu' \frac{\nu' \Delta\sigma_{\rm abs}(\nu')}{\nu'^2 - \nu^2}, \tag{6}$$

where ν_0 is the pion photoproduction threshold. Its low-energy expansion yields the following sum rules.

At the first order, one obtains the GDH sum rule,

$$I_{\rm GDH} \equiv \int_{\nu_0}^\infty \mathrm{d}\nu\, \frac{\Delta\sigma_{\rm abs}(\nu)}{\nu} = \frac{2\pi^2\alpha}{M^2}\kappa^2, \tag{7}$$

where κ is the anomalous magnetic moment of the nucleon. Substituting the proton mass M_p and the anomalous magnetic moment κ_p into the right-hand side, we obtain the GDH sum rule prediction quoted in the last row of Table II.

At the next two orders, one finds the FSP sum rules:

$$\gamma_0 = -\frac{1}{4\pi^2} \int_{\nu_0}^\infty \mathrm{d}\nu\, \frac{\Delta\sigma_{\rm abs}(\nu)}{\nu^3}, \tag{8}$$

$$\bar\gamma_0 = -\frac{1}{4\pi^2} \int_{\nu_0}^\infty \mathrm{d}\nu\, \frac{\Delta\sigma_{\rm abs}(\nu)}{\nu^5}\,. \tag{9}$$

In what follows, we assess the empirical helicity-difference cross section and evaluate $g(\nu)$, $I_{\rm GDH}$, γ_0, $\bar\gamma_0$ from the above integrals.

III. FIT OF THE POLARIZED PHOTOABSORPTION CROSS SECTION

We begin with performing a smooth fit of the experimental helicity-difference cross section of total photoabsorption on the proton. The fitting procedure is similar to the one applied for the unpolarized photoabsorption cross section $\sigma_{\rm abs}$ [4]. The integration domain is divided into three regions:

(i) *low energy*, $\nu \in [\nu_0\,,\ \nu_1)$;

(ii) *medium energy*, $\nu \in [\nu_1\,,\ 2\ \mathrm{GeV})$;

(iii) *high energy*, $\nu \in [2\ \mathrm{GeV}\,,\ \infty)$;

where ν_0 (≈ 0.145 GeV) and ν_1 (≈ 0.309 GeV) are thresholds for the single- and double-pion photoproduction, respectively. A smooth transition between the regions is implied.

In the *low-energy* region, we use the cross sections generated by MAID [20] (single-pion production only). Unfortunately, the MAID analysis does not provide any indication of its uncertainty. In our error estimate, we judiciously apply a 2% uncertainty to the MAID values.

In the *medium-energy* region, a fit to the data from the MAMI (Mainz) and ELSA (Bonn) experiments of the GDH and A2 collaborations [8–11] is applied in the form of a sum of six nonrelativistic Breit-Wigner resonances,

$$\Delta\sigma_{\rm res}(W) = \sum_{i=1}^{6} A_i\, \frac{\frac{1}{4}\Gamma_i^2}{(W - M_i)^2 + \frac{1}{4}\Gamma_i^2}, \tag{10}$$

where $W = \sqrt{s}$ is the invariant mass of the γp system. Widths (Γ), masses (M), and couplings (A) are treated as free fitting parameters. The resulting values are given in Table I.

In the *high-energy* region, a function of the following Regge form is used:

$$\Delta\sigma_{\rm Regge}(W) = C_1\, W^{p_1} + C_2\, W^{p_2}. \tag{11}$$

For W in GeV and the cross section in μb, we use the following fixed parameters [21]:

$$C_1 = -17.05 \pm 2.85\,, \quad C_2 = 104.7 \pm 14.5\,,$$
$$p_1 = -1.16 \pm 0.46\,, \quad p_2 = -3.32 \pm 0.44\,.$$

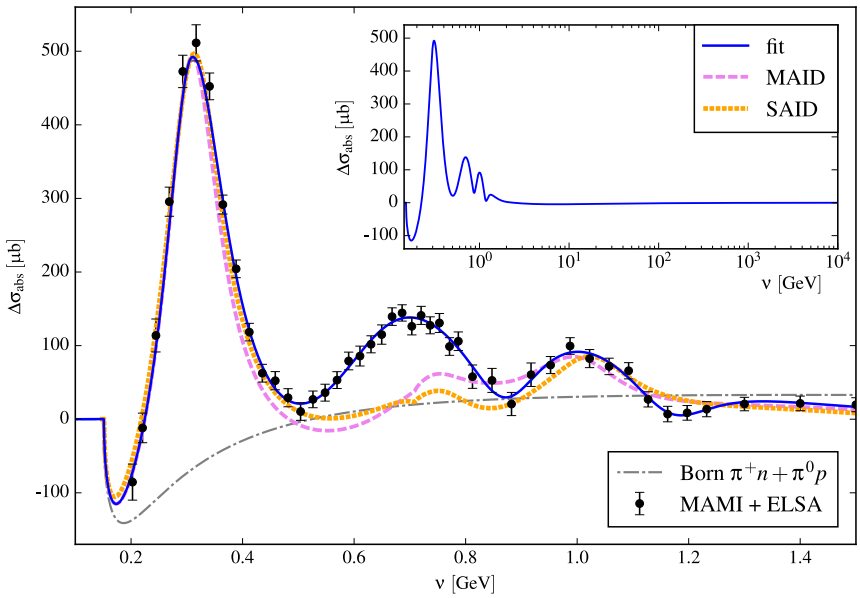

FIG. 1. Fit of experimental data for the helicity-difference cross section of total photoproduction on the proton. The solid curve shows our fit. The other curves, according to the legend, show the Born contribution (single-pion production on a pointlike proton), as well as the results of MAID [20] and SAID [25] multipole analyses.

TABLE I. Fitted resonances parameters entering Eq. (10).

i	M_i (MeV)	Γ_i (MeV)	$A_i \cdot \frac{1}{4}\Gamma_i^2$ (nb·GeV^2)
1	1210.2	119.3	1047.3
2	1405.0	493.5	−9008.4
3	1460.8	239.8	1964.0
4	1585.5	111.7	−226.9
5	1616.4	360.7	3829.3
6	1752.5	105.0	−103.4

The cross section fitting and the sum rule evaluations are accomplished with the help of the SciPy package for Python. We used the weighted nonlinear least-squares optimization procedure of SciPy's wrapper around minpack's lmdif and lmder algorithms. The latter implement the modified Levenberg-Marquardt algorithm [22, 23].

The resulting fit of the helicity-difference photoabsorption cross section is shown in Fig. 1. Also shown is the Born contribution for the $\pi^+n + \pi^0p$ photoproduction off a pointlike proton (with the vanishing anomalous magnetic moment), as well as the results of MAID [20] and SAID [25] multipole analyses.

IV. EVALUATION OF THE INTEGRALS

Having obtained the fit of the total photoproduction cross section, we proceed to the evaluation of the GDH and FSP sum rules, and ultimately of the forward CS amplitude. Our results for the sum rule integrals are presented in Table II, where they can be compared with some of the previous empirical evaluations, as well as the recent χPT results.

To estimate the uncertainty of our fits and dispersive integrals, we compute the covariance matrix of the fitted parameters. In the medium-energy region, the covariance matrix is simply obtained based on the experimental uncertainties of the data points. In the high-energy region, we make use of the uncertainties for the Regge parameters from Ref. [21], assuming that these four parameters are uncorrelated. We then apply the standard, linear error propagation to find the uncertainty of the dispersive integrals.

In the low-energy region, where the cross sections are not fit but obtained from the partial-wave analyses, we judiciously estimate the systematic error of each of the photoabsorption cross sections to be 2% of the magnitude of the unpolarized cross section, $\sigma(\nu)$. As the result, the error on $\Delta\sigma(\nu)$ is equal to 4% of $\sigma(\nu)$. This error is then linearly propagated to the dispersion integrals.

Within the calculated uncertainties, our evaluation appears to be consistent with the previous ones, as well as with the GDH sum rule value quoted in the bottom part of Table II. The discrepancy in the central value of the GDH integral can be traced back to the fact that our fit at the Δ-resonance peak happens to lie well below the central value of the data point; see Fig. 1. In particular, the GDH Collaboration [11] obtains $(254 \pm 5 \pm 12)$ μb in the interval of available data (i.e., $0.2 < \nu < 2.9$ GeV), while our fit of the same data yields (246.4 ± 6.8) μb.

Table III shows the contributions from each of the three energy regions. One can clearly see that the high-energy contribution is negligible for the FSPs. A more detailed behavior of the running sum rule integrals (functions of the cut-off — the upper integration bound) can be seen in Fig. 2. One can see the good convergence properties of all the integrals. It is interesting to observe the significant cancellations between the contribution below and above 0.2 GeV.

TABLE II. Empirical evaluations of the GDH and FSP integrals.

	$I_{\rm GDH}$ (μb)	γ_0 (10^{-6} fm^4)	$\bar\gamma_0$ (10^{-6} fm^6)
GDH & A2 [9, 11]	≈ 212	≈ -86	
Helbing [21]	$212 \pm 6 \pm 12$		
Bianchi-Thomas [24]	207 ± 23		
Pasquini *et al.* [12]	$210 \pm 6 \pm 14$	$-90 \pm 8 \pm 11$	$60 \pm 7 \pm 7$
This work	204.5 ± 21.4	-92.9 ± 10.5	48.4 ± 8.2
GDH sum rule	204.784481(4)[a]		
BχPT [15]		-90 ± 140	110 ± 50
HBχPT [17]		-260 ± 190	

[a] Right-hand side of Eq. (7) with CODATA [19] values of proton M and κ.

We note that the main contribution to the estimated uncertainty of the GDH integral comes from the high-energy Regge behavior, which is possibly both due to the fact that parameters seem to be not well "fixed" and because we have used a simplified covariance matrix estimation for these parameters. As for the higher-order sum rules, it appears that the main contribution to the uncertainty comes from our assumption about the systematic uncertainty of the partial-wave analyses (low-energy region).

TABLE III. Contributions to the GDH and FSP integrals by regions.

Sum Rule \ Region	*low-energy*	*medium-energy*	*high-energy*
$I_{\rm GDH}$ (μb)	43.6 ± 6.0	175.7 ± 3.7	-14.8 ± 19.9
γ_0 (10^{-6} fm^4)	3.6 ± 10.3	-96.5 ± 2.0	$(2 \pm 7) \times 10^{-2}$
$\bar\gamma_0$ (10^{-6} fm^6)	77.1 ± 8.2	-28.7 ± 0.6	$(2 \pm 36) \times 10^{-5}$

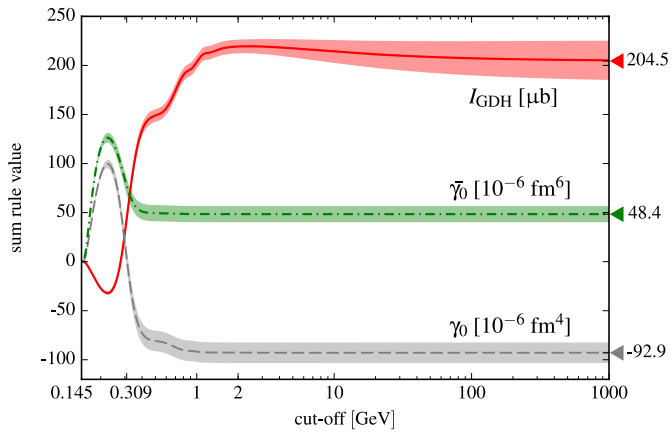

FIG. 2. The GDH and FSP integrals as a function of the upper integration bound. Bands represent estimated errors. Asymptotic values of the integrals are displayed on the right and marked with colored triangles.

We next evaluate the entire spin-dependent amplitude $g(\nu)$. In order to improve on the accuracy, we use the subtracted dispersion relation:

$$\mathrm{Re}\, g(\nu) = -\frac{\alpha\kappa^2}{2M^2}\nu - \frac{\nu^3}{4\pi^2}\fint_{\nu_0}^{\infty} \mathrm{d}\nu' \, \frac{\Delta\sigma_{\rm abs}(\nu')}{(\nu'^2 - \nu^2)\,\nu'}. \quad (12)$$

The only difference with the unsubtracted one, Eq. (6), is accuracy. Indeed, the subtraction replaces the value of the GDH integral (see "This work" in Table II) by the much more accurate GDH sum rule value (next row) and leads to the smaller uncertainty.

The remaining integral in Eq. (12) converges very fast in the considered energy range. The resulting amplitude is plotted in Fig. 3. The upper panel shows the real and imaginary parts in the energy range where the data (for the imaginary part) are available.

The lower panel of Fig. 3 zooms into the lower energy range where our results can be compared with next-next-to-leading order χPT calculations of Lensky *et al.* [15]. One notes here that the imaginary parts differ appreciably at energies around 0.25 GeV. Nevertheless, their integrals (i.e., the real parts) agree perfectly at low ν. This is a "scientific miracle" of the effective field theory — the low-energy quantities are well described, even though they are obtained as loop or dispersive integrals which include higher-energy domains where the theory is inapplicable.

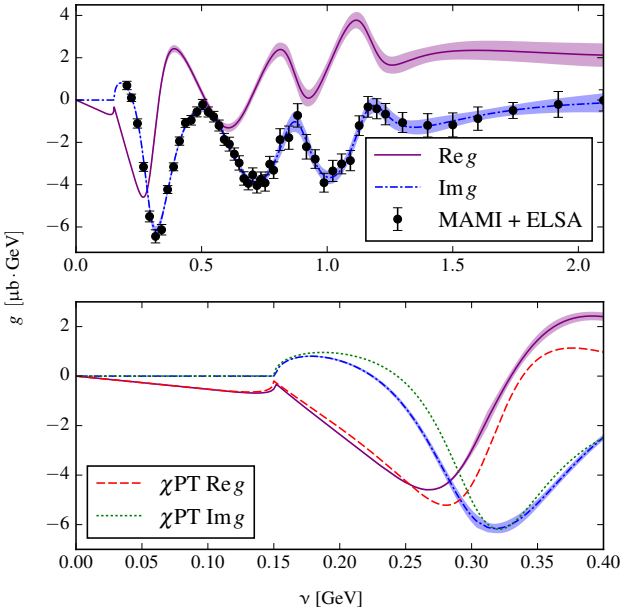

FIG. 3. Spin-dependent amplitude $g(\nu)$ obtained from numerical integration of the fit of data for the helicity-difference photoproduction cross section. Dashed and dotted curves in the bottom panel are the BχPT predictions of Ref. [15]. Bands represent the error estimate.

V. OBSERVABLES

Given both amplitudes, $f(\nu)$ and $g(\nu)$, one can reconstruct the energy dependence of the forward CS observables. The differential cross section of the forward CS in the laboratory

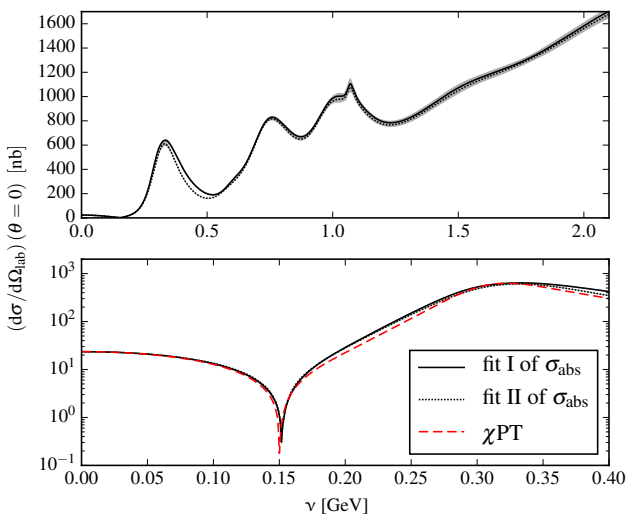

FIG. 4. Differential cross section of the forward CS off the proton for the two distinctive fits of the unpolarized photoabsorption cross section, obtained in Ref. [4]. The solid gray band represents the resulting estimated uncertainty on the observable. The red dashed curve shows the BχPT calculation of Ref. [15].

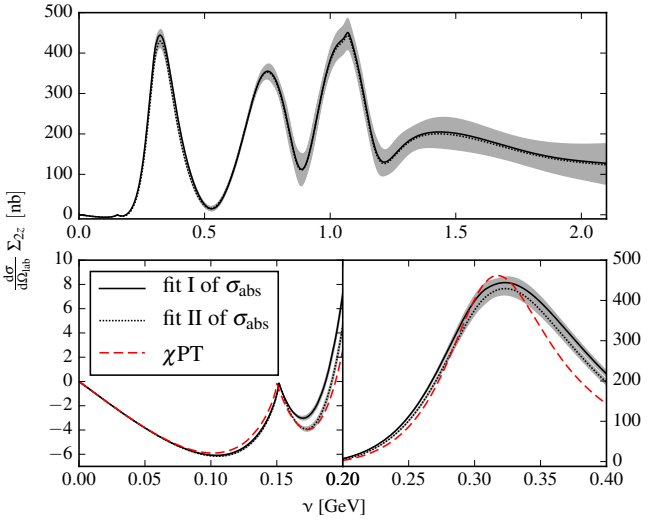

FIG. 5. Unpolarized differential cross section multiplied with Σ_{2z}-asymmetry for the forward CS off the proton. The two distinctive fits of the unpolarized photoabsorption cross section are obtained in Ref. [4]. The solid gray band represents the resulting estimated uncertainty on the observable. The red dashed curve shows the BχPT calculation of Ref. [15].

frame is expressed as follows:

$$\left.\frac{\mathrm{d}\sigma}{\mathrm{d}\Omega_{\mathrm{lab}}}\right|_{\theta=0} = |f|^2 + |g|^2. \tag{13}$$

The other nonvanishing observables involve the photon and nucleon spin polarization along the z axis. When only the initial particles are polarized, the corresponding asymmetry is known as Σ_{2z} and can be defined as

$$\Sigma_{2z} = \frac{\mathrm{d}\sigma_{3/2} - \mathrm{d}\sigma_{1/2}}{\mathrm{d}\sigma_{3/2} + \mathrm{d}\sigma_{1/2}}, \tag{14}$$

where σ_Λ denotes the doubly polarized CS cross section with Λ being the combined helicity of the initial state. When the initial photon and the final nucleon are polarized, the asymmetry is called $\Sigma_{2z'}$. For the forward scattering, all asymmetries involving such pairwise polarization are equal and in terms of f and g are given as follows:

$$\Sigma_{2z}\big|_{\theta=0} = -\frac{2\,\mathrm{Re}(fg^*)}{|f|^2 + |g|^2}. \tag{15}$$

In Table IV, we list the empirical values of the real part of the forward amplitudes $f(\nu)$ and $g(\nu)$ for several values of ν; for other values, see Ref. [26]. Below the pion-production threshold ($\nu < m_\pi + m_\pi^2/2M_p$), where the amplitudes are real, the observables can simply be obtained by substituting these values in Eq. (13) and (15). Above the pion threshold, one obviously needs the photoabsorption cross sections [cf. Eq. (4)], which we include in the Supplemental Material [26].

The resulting unpolarized and helicity-difference CS differential cross sections at zero angle are shown in Figs. 4 and 5, respectively. The lower panels show the comparison with χPT predictions at lower energies. Note the logarithmic scale in the case of the unpolarized cross section, Fig. 4 (lower panel). Incidentally, both f and g amplitudes happen to nearly vanish at the pion-production threshold, and so do the cross sections.

The error estimation for the observables is accomplished with the same basic approach as for the case of dispersion integrals, described above. We account for the uncertainty contribution of both f and g.

Once again, a remarkable agreement with the χPT calculations at low energies is observed. For the case of the beam asymmetry, however, the cusp at $\nu \approx 151.5$ MeV, caused by the second pion production threshold (namely the $\pi^+ n$ channel), appears to be somewhat sharper than the one obtained within χPT. This is mainly because the neutral and charged pion production thresholds coincide in the χPT calculation due to unbroken isospin symmetry.

VI. CONCLUSION

We have obtained a first complete model-independent evaluation of the forward Compton scattering off the proton. Our results are based on dispersive sum rules for which the empirical total photoabsorption cross sections serve as input. Putting together the fits of the unpolarized photoabsorption cross section obtained earlier [4] and the helicity-difference cross section obtained here, we have computed the sum rule integrals as well as the energy dependence of the forward CS amplitudes.

The existing database for the helicity-difference photoabsorption cross section ($\Delta\sigma_{\mathrm{abs}}$) is not as comprehensive as for the unpolarized cross section (σ_{abs}). It consists of only the MAMI (Mainz) and ELSA (Bonn) experimental data between 0.2 and 2.9 GeV. Nevertheless, it proved to be sufficient for a reliable evaluation of the spin-dependent amplitude, and subsequently the observables, for photon lab energies up to

TABLE IV. Empirical values of the forward amplitudes for proton CS in units of μb · GeV.

ν (MeV)	Re $f_{(\text{fit I})}$	Re $f_{(\text{fit II})}$	Re g
50	-2.84 ± 0.01	-2.85 ± 0.01	-0.26 ± 0.01
60	-2.76 ± 0.01	-2.76 ± 0.01	-0.32 ± 0.01
70	-2.65 ± 0.01	-2.66 ± 0.01	-0.37 ± 0.01
79	-2.54 ± 0.01	-2.56 ± 0.01	-0.42 ± 0.01
90	-2.38 ± 0.01	-2.40 ± 0.01	-0.48 ± 0.01
100	-2.21 ± 0.01	-2.23 ± 0.01	-0.54 ± 0.01
110	-2.00 ± 0.01	-2.03 ± 0.01	-0.59 ± 0.01
120	-1.75 ± 0.01	-1.78 ± 0.01	-0.64 ± 0.01
130	-1.45 ± 0.02	-1.48 ± 0.02	-0.68 ± 0.01
135	-1.27 ± 0.02	-1.30 ± 0.02	-0.69 ± 0.01
145	-0.79 ± 0.03	-0.83 ± 0.03	-0.65 ± 0.02
150	-0.39 ± 0.03	-0.42 ± 0.03	-0.52 ± 0.02
160	0.04 ± 0.04	0.00 ± 0.04	-0.68 ± 0.03
180	0.48 ± 0.04	0.34 ± 0.04	-1.53 ± 0.03
200	1.13 ± 0.04	0.92 ± 0.04	-2.35 ± 0.03
225	2.25 ± 0.05	1.94 ± 0.05	-3.38 ± 0.03
245	3.29 ± 0.05	2.87 ± 0.05	-4.14 ± 0.03
265	4.09 ± 0.04	3.55 ± 0.05	-4.59 ± 0.03
275	4.14 ± 0.03	3.58 ± 0.04	-4.53 ± 0.03
300	2.15 ± 0.14	1.82 ± 0.16	-3.00 ± 0.18
325	-2.00 ± 0.22	-2.41 ± 0.24	-0.44 ± 0.22
440	-7.12 ± 0.16	-6.27 ± 0.11	1.81 ± 0.15
580	-2.93 ± 0.18	-2.47 ± 0.11	-1.18 ± 0.19
750	-7.12 ± 0.14	-6.63 ± 0.13	1.45 ± 0.25
1000	-9.73 ± 0.19	-9.32 ± 0.19	1.46 ± 0.36
2200	-10.35 ± 0.21	-9.97 ± 0.21	2.10 ± 0.55

several GeV. The influence of the experimentally unknown high-energy behavior of the helicity-difference cross section is largely diminished by using a subtraction in the form of the GDH sum rule, cf. Eq. (12).

Considering the low-energy expansion of the forward spin-dependent amplitude, we have (re)evaluated the GDH integral and the two first forward spin polarizabilities. These results are in agreement with the previous evaluations, cf. Table II.

As explained in the Introduction, it is very difficult to access the forward CS experimentally. Most of the CS data for the proton are in fact obtained at scattering angles of 90 deg and above. On the other hand, the relation of the forward CS to the photoabsorption data exploited here is exact, and this sort of evaluation is the next best thing to the real CS data. In some aspects, it is even better (e.g., accuracy and costs). The main advantage is that we directly access the amplitudes, rather than observables, and hence one has, for example, simpler (linear, rather than bilinear) constraints on the multipole amplitudes. The multipole analysis of the proton CS data using the stringent constraints of the forward scattering is a subject for near-future work.

ACKNOWLEDGMENTS

This work was supported by the Deutsche Forschungsgemeinschaft through the Collaborative Research Center SFB 1044 [The Low-Energy Frontier of the Standard Model] and the Graduate School DFG/GRK 1581 [Symmetry Breaking in Fundamental Interactions].

Appendix A: Sum rules for elastic contribution in spinor QED

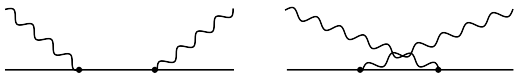

FIG. 6. Tree-level CS graphs.

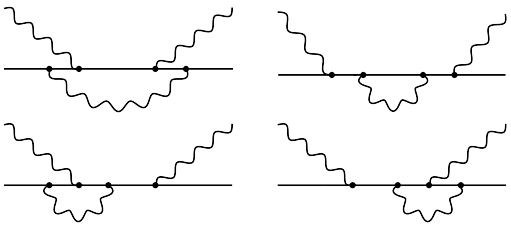

FIG. 7. One-loop graphs contributing to the forward CS. Graphs obtained from these by crossing of the photon lines are included, too.

Let us examine the CS (elastic) contribution to the sum rules in spinor QED at $O(\alpha^2)$. Consider the scattering of a photon from a charged spin-1/2 particle with mass M. The helicity amplitudes are expressed in terms of the Feynman amplitude as

$$T_{\lambda'_\gamma \lambda'_N \lambda_\gamma \lambda_N} = \bar{u}_{\lambda'_N}(\boldsymbol{p}')\, \varepsilon^*_{\lambda'_\gamma}(q') \cdot T(q', q, p', p) \cdot \varepsilon_{\lambda_\gamma}(q)\, u_{\lambda_N}(\boldsymbol{p})\,,$$

where we denote the helicity and 4-momentum of the incoming (outgoing) photon by $\lambda_\gamma(\lambda'_\gamma)$ and $q(q')$ and the helicity and momentum of the incoming (outgoing) spin-1/2 particle by $\lambda_N(\lambda'_N)$ and $p(p')$. The spinors are normalized according to

$$\bar{u}_{\lambda'_N}(\boldsymbol{p})\, u_{\lambda_N}(\boldsymbol{p}) = \delta_{\lambda'_N \lambda_N}\,, \tag{A1}$$

where $\boldsymbol{p}$ is the nucleon 3-momentum. In general, there are six independent helicity amplitudes for the CS process. The $O(\alpha^2)$ unpolarized and double-polarized cross sections [27] can be deduced from the tree-level helicity amplitudes [28, 29],

$$\sigma^{(2)} = \frac{2\pi\alpha^2}{M^2}\left\{\frac{1+x}{x^3}\left[\frac{2x(1+x)}{1+2x} - \ln(1+2x)\right] + \frac{1}{2x}\ln(1+2x) - \frac{1+3x}{(1+2x)^2}\right\}, \tag{A2a}$$

$$\Delta\sigma^{(2)} = -\frac{2\pi\alpha^2}{M^2 x}\left\{\left[1+\frac{1}{x}\right]\ln(1+2x) - 2\left[1+\frac{x^2}{(1+2x)^2}\right]\right\}, \tag{A2b}$$

with $x = \nu/M$. We note that in the low-energy limit the total unpolarized cross section, σ, reproduces the Thomson cross section, $\sigma^{(2)}(0) = 8\pi\alpha^2/3M^2$, a result that is unaltered by loop corrections. In the same limit, the helicity-difference cross section, $\Delta\sigma$, is vanishing.

In the forward limit, only two helicity amplitudes are nonvanishing. These are the amplitudes without spin flip: $T_{+1\,+1/2\,+1\,+1/2}$ and $T_{-1\,+1/2\,-1\,+1/2}$. They can be used to reconstruct the spin-dependent and spin-independent forward CS amplitudes:

$$f = \frac{1}{2}\left[T_{+1\,+1/2\,+1\,+1/2} + T_{-1\,+1/2\,-1\,+1/2}\right], \tag{A3a}$$

$$g = \frac{1}{2}\left[T_{+1\,+1/2\,+1\,+1/2} - T_{-1\,+1/2\,-1\,+1/2}\right]. \tag{A3b}$$

At tree level (Fig. 6), the spinor QED calculation yields $f^{(1)}(\nu) = -\alpha/M$ and $g^{(1)}(\nu) = 0$, where the superscript indicates the order of α. Next, we consider the one-loop corrections (Fig. 7). Tsai *et al.* [28, 29] calculated the Compton scattering helicity amplitudes up to $O(\alpha^2)$. From their result, we obtain the forward CS amplitudes:

$$f^{(2)}(x) = \frac{\alpha^2}{4\pi M}\left\{\frac{24x^2\left(1-3x^2\right)+\pi^2\left(4x^4+8x^3-9x^2-2x+2\right)}{6x^2\left(1-4x^2\right)} - \frac{4x^2\left(4x^2-3\right)}{\left(4x^2-1\right)^2}\ln 2x\right. \tag{A4a}$$
$$\left. -\frac{x^2-2x-2}{x^2}\left[\ln 2x\ln(1+2x)+\mathrm{Li}_2\left(-2x\right)\right] + \frac{x^2+2x-2}{x^2}\mathrm{Li}_2\left(1-2x\right)\right\} + \frac{iMx}{4\pi}\sigma^{(2)}(x),$$

$$g^{(2)}(x) = \frac{\alpha^2}{4\pi M}\left\{\frac{12x^2+\pi^2\left(4x^3-4x^2-x+1\right)}{6x\left(4x^2-1\right)} - \frac{16x^3}{\left(4x^2-1\right)^2}\ln 2x\right. \tag{A4b}$$
$$\left. -\frac{x+1}{x}\left[\ln 2x\ln(1+2x)+\mathrm{Li}_2\left(-2x\right)\right] - \frac{x-1}{x}\mathrm{Li}_2\left(1-2x\right)\right\} - \frac{iMx}{8\pi}\Delta\sigma^{(2)}(x).$$

The fact that $\mathrm{Im}\, f^{(2)}(\nu) = \nu\,\sigma^{(2)}(\nu)/4\pi$ and $\mathrm{Im}\, g^{(2)}(\nu) = -\nu\,\Delta\sigma^{(2)}(\nu)/8\pi$ is in accordance with the optical theorem, cf. Eq. (4). Also, we have checked that the one-loop amplitudes indeed satisfy the dispersion relations:

$$f^{(2)}(\nu) = \frac{2\nu^2}{\pi}\int_0^\infty \mathrm{d}\nu'\,\frac{\mathrm{Im}\, f^{(2)}(\nu')}{\nu'\left(\nu'^2-\nu^2-i0^+\right)}, \tag{A5a}$$

$$g^{(2)}(\nu) = \frac{2\nu}{\pi}\int_0^\infty \mathrm{d}\nu'\,\frac{\mathrm{Im}\, g^{(2)}(\nu')}{\nu'^2-\nu^2-i0^+}, \tag{A5b}$$

where the subtraction in Eq. (A5a) corresponds to $f^{(2)}(0) = 0$.

Now, we want to understand the low-energy expansion, and thus the polarizability sum rules in spinor QED. In Ref. [4], we already performed this exercise in scalar QED. Expanding the real part of Eq. (A5) around $\nu = 0$, we find

$$\frac{\alpha^2}{\pi M}\left(\frac{11+48\ln\frac{2\nu}{M}}{18M^2}\nu^2 + \frac{7(257+1140\ln\frac{2\nu}{M})}{450M^4}\nu^4 + \frac{68(107+672\ln\frac{2\nu}{M})}{441M^6}\nu^6 + \ldots\right) = \frac{1}{2\pi^2}\sum_{n=1}^\infty \nu^{2n}\int_0^\infty \mathrm{d}\nu'\,\frac{\sigma^{(2)}(\nu')}{\nu'^{\,2n}},$$

$$\frac{\alpha^2}{\pi M}\left(\frac{37+60\ln\frac{2\nu}{M}}{18M^3}\nu^3 + \frac{64(29+105\ln\frac{2\nu}{M})}{225M^5}\nu^5 + \frac{18(89+504\ln\frac{2\nu}{M})}{49M^7}\nu^7 + \ldots\right) = \frac{1}{4\pi^2}\sum_{n=1}^\infty \nu^{2n-1}\int_0^\infty \mathrm{d}\nu'\,\frac{\Delta\sigma^{(2)}(\nu')}{\nu'^{\,2n-1}}.$$

Hence, the coefficients diverge in the infrared. However, there is an apparent mismatch: they are logarithmically divergent on one side and power divergent on the other. To match the sides exactly at each order of ν, thus defining the sum rules for "quasistatic" polarizabilities, we subtract all the power divergences on the right-hand-side (rhs) and regularize both sides with the same infrared cutoff (equal to ν):

$$\frac{\alpha^2}{\pi M}\left(\frac{11+48\ln\frac{2\nu}{M}}{18M^2}\nu^2 + \frac{7(257+1140\ln\frac{2\nu}{M})}{450M^4}\nu^4 + \ldots\right) = \frac{1}{2\pi^2}\sum_{n=1}^\infty \nu^{2n}\int_\nu^\infty \mathrm{d}\nu'\,\frac{\sigma^{(2)}(\nu') - \sum_{k=0}^{2(n-1)}\frac{1}{k!}\frac{\mathrm{d}^k\sigma^{(2)}(\nu)}{\mathrm{d}\nu^k}\Big|_{\nu=0}\nu'^{\,k}}{\nu'^{\,2n}},$$

$$\frac{\alpha^2}{\pi M}\left(\frac{37+60\ln\frac{2\nu}{M}}{18M^3}\nu^3 + \frac{64(29+105\ln\frac{2\nu}{M})}{225M^5}\nu^5 + \ldots\right) = \frac{1}{4\pi^2}\sum_{n=2}^\infty \nu^{2n-1}\int_\nu^\infty \mathrm{d}\nu'\,\frac{\Delta\sigma^{(2)}(\nu') - \sum_{k=0}^{2n-3}\frac{1}{k!}\frac{\mathrm{d}^k\Delta\sigma^{(2)}(\nu)}{\mathrm{d}\nu^k}\Big|_{\nu=0}\nu'^{\,k}}{\nu'^{\,2n-1}}.$$

Both sides are now identical at each order of ν. This is nontrivial, at least for the analytic terms; the logs are fairly easily obtained from the nonregularized rhs of the low-energy expanded dispersion relation, cf. Ref. [27]. Since the GDH sum rule only differs from zero starting from $O(\alpha^3)$, we omitted the $O(\nu)$ term in the last equation.

Extending these arguments to all orders in α, we find that the proper low-energy expansion for the "elastic" part of the amplitudes reads as

$$f_{\rm el}(\nu) = -\frac{\alpha}{M} + \frac{1}{2\pi^2}\sum_{n=1}^{\infty}\nu^{2n}\int_\nu^\infty \mathrm{d}\nu'\,\frac{\sigma(\nu')-\overline{\sigma}_n(\nu')}{\nu'^{\,2n}}\,, \tag{A6a}$$

$$g_{\rm el}(\nu) = \frac{1}{4\pi^2}\sum_{n=1}^{\infty}\nu^{2n-1}\int_\nu^\infty \mathrm{d}\nu'\,\frac{\Delta\sigma(\nu')-\overline{\Delta\sigma}_n(\nu')}{\nu'^{\,2n-1}}\,, \tag{A6b}$$

where the bar denotes the infrared subtractions:

$$\overline{\sigma}_n(\nu') \equiv \sum_{k=0}^{2(n-1)} \frac{1}{k!}\frac{\mathrm{d}^k\sigma(\nu)}{\mathrm{d}\nu^k}\Big|_{\nu=0}\nu'^{\,k}, \tag{A7a}$$

$$\overline{\Delta\sigma}_n(\nu') \equiv \begin{cases} 0 & n=1 \\ \sum\limits_{k=0}^{2n-3} \frac{1}{k!}\frac{\mathrm{d}^k\Delta\sigma(\nu)}{\mathrm{d}\nu^k}\Big|_{\nu=0}\nu'^{\,k} & n>1. \end{cases} \tag{A7b}$$

Accordingly, the elastic contributions to the polarizabilities are given by

$$(\alpha_{E1}+\beta_{M1})_{\rm el} = \frac{1}{2\pi^2}\int_\nu^\infty \mathrm{d}\nu'\,\frac{\sigma(\nu')-\sigma(0)}{\nu'^{\,2}}, \tag{A8a}$$

$$(\gamma_0)_{\rm el} = -\frac{1}{4\pi^2}\int_\nu^\infty \mathrm{d}\nu'\,\frac{\Delta\sigma(\nu')-\overline{\Delta\sigma}_2(0)}{\nu'^{\,3}}, \tag{A8b}$$

$$(\bar{\gamma}_0)_{\rm el} = -\frac{1}{4\pi^2}\int_\nu^\infty \mathrm{d}\nu'\,\frac{\Delta\sigma(\nu')-\overline{\Delta\sigma}_3(0)}{\nu'^{\,5}}. \tag{A8c}$$

In our one-loop spinor QED example, plugging in the tree-level cross sections from Eq. (A2), we obtain

$$(\alpha_{E1}+\beta_{M1})_{\rm el} = \frac{\alpha^2}{18\pi M^3}\left(11+48\ln\frac{2\nu}{M}\right), \tag{A9a}$$

$$(\gamma_0)_{\rm el} = -\frac{\alpha^2}{18\pi M^4}\left(37+60\ln\frac{2\nu}{M}\right), \tag{A9b}$$

$$(\bar{\gamma}_0)_{\rm el} = -\frac{64\,\alpha^2}{225\pi M^6}\left(29+105\ln\frac{2\nu}{M}\right), \tag{A9c}$$

which obviously matches the corresponding terms in the low-energy expansion of the tree-level amplitudes.

[1] M. Gell-Mann, M. L. Goldberger and W. E. Thirring, "Use of causality conditions in quantum theory," Phys. Rev. **95**, 1612 (1954).

[2] D. Drechsel, B. Pasquini and M. Vanderhaeghen, "Dispersion relations in real and virtual Compton scattering," Phys. Rept. **378**, 99 (2003).

[3] F. Hagelstein, R. Miskimen and V. Pascalutsa, "Nucleon Polarizabilities: from Compton Scattering to Hydrogen Atom," Prog. Part. Nucl. Phys. **88**, 29 (2016).

[4] O. Gryniuk, F. Hagelstein and V. Pascalutsa, "Evaluation of the forward Compton scattering off protons: Spin-independent amplitude," Phys. Rev. D **92**, 074031 (2015).

[5] H. Alvensleben *et al.*, Phys. Rev. Lett. **30**, 328 (1973).

[6] S. B. Gerasimov, "A Sum rule for magnetic moments and the damping of the nucleon magnetic moment in nuclei," Sov. J. Nucl. Phys. **2**, 430 (1966) [Yad. Fiz. **2**, 598 (1965)].

[7] S. D. Drell and A. C. Hearn, "Exact Sum Rule for Nucleon Magnetic Moments," Phys. Rev. Lett. **16** (1966) 908.

[8] J. Ahrens *et al.* [GDH and A2 Collaborations], "Helicity dependence of gamma p $\to$ N pi below 450-MeV and contribution to the Gerasimov-Drell-Hearn sum rule," Phys. Rev. Lett. **84** (2000) 5950.

[9] J. Ahrens *et al.* [GDH and A2 Collaborations], "First measurement of the Gerasimov-Drell-Hearn integral for Hydrogen from 200 to 800 MeV," Phys. Rev. Lett. **87** 022003, (2001).

[10] H. Dutz *et al.* [GDH Collaboration], "First measurement of the Gerasimov-Drell-Hearn sum rule for H-1 from 0.7-GeV to 1.8-GeV at ELSA," Phys. Rev. Lett. **91**, 192001 (2003).

[11] H. Dutz *et al.*, "Experimental Check of the Gerasimov-Drell-Hearn Sum Rule for H-1," Phys. Rev. Lett. **93**, 032003 (2004).

[12] B. Pasquini, P. Pedroni and D. Drechsel, "Higher order forward spin polarizability," Phys. Lett. B **687**, 160 (2010).

[13] V. Lensky and V. Pascalutsa, "Manifestly-covariant chiral PT calculation of nucleon Compton scattering," Pisma Zh. Eksp. Teor. Fiz. **89**, 127 (2009) [JETP Lett. **89**, 108 (2009)]. arXiv:0803.4115 [nucl-th].

[14] V. Lensky and V. Pascalutsa, "Predictive powers of chiral perturbation theory in Compton scattering off protons," Eur. Phys. J. C **65**, 195 (2010).

[15] V. Lensky, J. McGovern and V. Pascalutsa, "Predictions of covariant chiral perturbation theory for nucleon polarisabilities and polarised Compton scattering," Eur. Phys. J. C **75**, no. 12, 604 (2015).

[16] H. W. Grießhammer, J. A. McGovern, D. R. Phillips and G. Feldman, "Using effective field theory to analyse low-energy Compton scattering data from protons and light nuclei," Prog. Part. Nucl. Phys. **67**, 841 (2012). arXiv:1203.6834 [nucl-th].

[17] J. A. McGovern, D. R. Phillips and H. W. Grießhammer, "Compton scattering from the proton in an effective field theory with explicit Delta degrees of freedom," Eur. Phys. J. A **49**, 12 (2013). arXiv:1210.4104 [nucl-th].

[18] V. Lensky, J. A. McGovern, D. R. Phillips and V. Pascalutsa, "What different variants of chiral EFT predict for the proton Compton differential cross section - and why," Phys. Rev. C **86**, 048201 (2012). arXiv:1208.4559 [nucl-th].

[19] P. J. Mohr, B. N. Taylor, and D. B. Newell, "The 2014 CODATA

Recommended Values of the Fundamental Physical Constants" (Web Version 7.0). [http://physics.nist.gov/constants]

[20] D. Drechsel, S. S. Kamalov and L. Tiator, Eur. Phys. J. A **34**, 69 (2007) (MAID program: http://www.kph.uni-mainz.de/MAID/)

[21] K. Helbing, "The Gerasimov-Drell-Hearn Sum Rule," Prog. Part. Nucl. Phys. **57**, 405 (2006).

[22] K. Levenberg. "A Method for the Solution of Certain Non-Linear Problems in Least Squares," Q. Appl. Math., 2: 164-168 (1944).

[23] D. W. Marquardt. "An algorithm for least-squares estimation of nonlinear parameters," J. Soc. Ind. Appl. Math., 11(2): 431-441 (1963).

[24] N. Bianchi and E. Thomas, "Parameterization of [sigma(1/2) - sigma(3/2)] for $Q^2 \geq 0$ and nonresonance contribution to the GDH sum rule," Phys. Lett. B **450**, 439 (1999).

[25] R. L. Workman, M. W. Paris, W. J. Briscoe, and W. J. Strakovsky, Phys. Rev. C **86**, 015202 (2012) (SAID program: http://gwdac.phys.gwu.edu)

[26] See Supplemented Material for the numerical values of the resulting forward amplitudes and observables of proton CS.

[27] B. R. Holstein, V. Pascalutsa and M. Vanderhaeghen, "Sum rules for magnetic moments and polarizabilities in QED and chiral effective-field theory," Phys. Rev. **D** 72, 094014 (2005).

[28] W.-Y. Tsai, L. L Deraad and K. A. Milton, "Compton scattering. ii. differential cross-sections and left-right asymmetry," Phys. Rev. D **6**, 1428 (1972) [Erratum: Phys. Rev. D **11** (1975) 703].

[29] K. A. Milton, W.-Y. Tsai and L. L Deraad, "Compton scattering. i. spectral forms for the invariant amplitudes to order e-to-the-4," Phys. Rev. D **6**, 1411 (1972).